Intermittent reconnection and plasmoids in UV bursts in the low solar atmosphere

Luc Rouppe van der Voort[1,2], Bart De Pontieu[3,1,2], Göran Scharmer[4,5], Jaime de la Cruz Rodríguez[4], Juan Martínez-Sykora[3,6], Daniel Nóbrega-Siverio[7,8], Lijia Guo[3,6], Shahin Jafarzadeh[1,2], Tiago Pereira[1,2], Viggo Hansteen[1,2], Mats Carlsson[1,2], Gregal Vissers[4]

[1]Rosseland Centre for Solar Physics, University of Oslo, [2]Institute of Theoretical Astrophysics, University of Oslo, [3]Lockheed Martin Solar & Astrophysics Lab, Palo Alto, [4]Institute for Solar Physics, Department of Astronomy, Stockholm University, [5]Royal Swedish Academy of Sciences, [6]Bay Area Environmental Research Institute, [7]Instituto de Astrofísica de Canarias, La Laguna, [8]Department of Astrophysics, Universidad de La Laguna

(published in ApJ Letters 2017 Vol. 851 L6, arXiv:1711.04581)

Summary

Magnetic reconnection is thought to drive a wide variety of dynamic phenomena in the solar atmosphere. Yet the detailed physical mechanisms driving reconnection are difficult to discern in the remote sensing observations that are used to study the solar atmosphere. We exploit the high-resolution instruments Interface Region Imaging Spectrograph (IRIS) and the new CHROMIS Fabry-Perot instrument at the Swedish 1-m Solar Telescope (SST) to identify the intermittency of magnetic reconnection and its association with the formation of plasmoids in so-called UV bursts in the low solar atmosphere.

Fig. 2 and 3: The Si IV 1403Å UV burst spectra from the transition region show evidence of highly broadened line profiles with often non-Gaussian and triangular shapes, in addition to signatures of bidirectional flows. Such profiles had previously been linked, in idealized numerical simulations, to magnetic reconnection driven by the plasmoid instability (see e.g. Innes et al. 2015 and Guo et al. 2018).

Fig. 1: Simultaneous CHROMIS images in the chromospheric Ca II K 3934Å line now provide compelling evidence for the presence of plasmoids, by revealing highly dynamic and rapidly moving brightenings that are smaller than 0.2 arcsec and that evolve on timescales of order seconds.

Fig. 4: Our interpretation of the observations is supported by detailed comparisons with synthetic observables from advanced numerical simulations of magnetic reconnection and associated plasmoids in the chromosphere.

Our results highlight how subarcsecond imaging spectroscopy sensitive to a wide range of temperatures combined with advanced numerical simulations that are realistic enough to compare with observations can directly reveal the small-scale physical processes that drive the wide range of phenomena in the solar atmosphere.

References:

Guo et al. 2018, submitted
Innes et al. 2015, ApJ, 813, 86
Nóbrega-Siverio et al. 2017, ApJ, 850, 153
Peter et al. 2014, Science, 346, 1255726
Rouppe van der Voort et al. 2017 ApJ 851 L6
Vissers et al. 2015, ApJ, 812, 11
Young et al. 2018, arXiv:1805.05850

Scan the QR code or go to
http://folk.uio.no/rouppe/plasmoids_chromis/
to view movies

Fig. 1: In UV bursts, Ca II K wing images show small and rapidly evolving blobs → plasmoids?

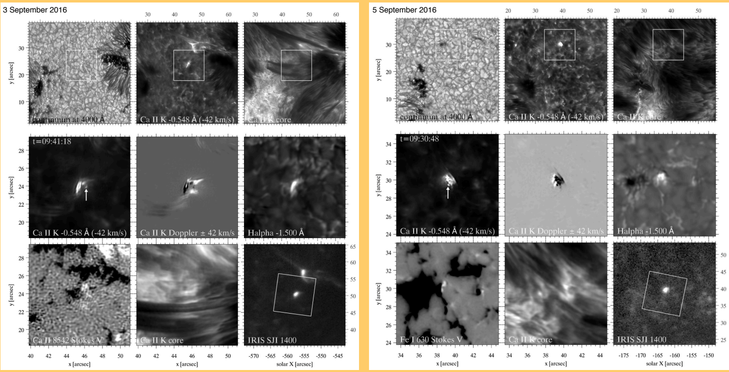

Different imaging diagnostics for the two datasets. The top row shows large FOV overview images. The white box in the top row and the IRIS SJI 1400 image in the lower right marks the area centered on the UV burst shown in more detail in the SST images in the bottom rows. All images are shown with coordinates of the CHROMIS FOV, except the IRIS SJI 1400 image, which has heliocentric-cartesian coordinates. The white arrow marks an isolated plasmoid-like blob. Scan the QR code on this poster or go to http://folk.uio.no/rouppe/plasmoids_chromis/ to view movies of the bottom two rows. ***The rapidly evolving blobs are most obvious in the movies.***

Fig. 4: Bifrost simulations show plasmoids in reconnection regions. Synthetic Si IV and Ca II spectral profiles resemble the IRIS and CHROMIS observations

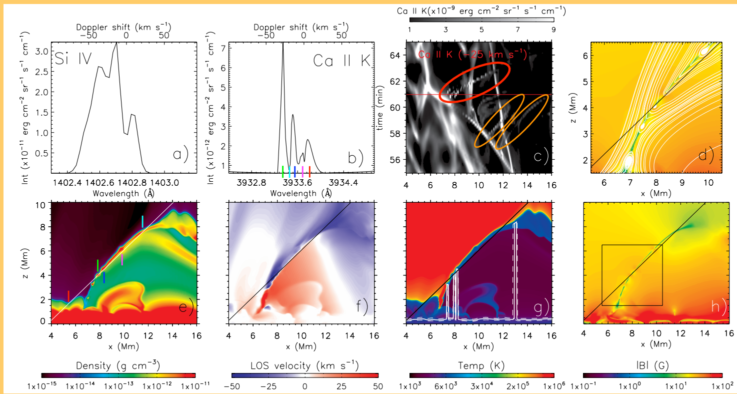

Results from the 2.5D Bifrost simulation. Synthetic spectral profiles of Si IV (a) and Ca II (b) computed along the inclined line shown in panels (d)–(h) which crosses some plasmoids. Panel (c) shows the space-time plot of Ca II blue wing (25 km/s) with the LOS along the vertical axis. The red horizontal line is marking the time of the other panels. Maps of the density, velocity along the inclined LOS, and temperature are shown in panels (e), (f) and (g). The white contours in panel (g) mark the heights of $\tau = 0.3,1,3$ along the vertical LOS for the −25 km/s blue wing of Ca II K. Panels (d) and (h) show the absolute magnitude of the magnetic field, with (d) zooming in on plasmoids which can be recognized as magnetic islands by selected field lines (white contours). The plasmoids are readily seen in the density map and correspond to very narrow Ca II brightenings that travel from left to right in panel (c) and are high-lighted by ellipses: the red ellipse marks the plasmoids that produced the Ca II K profile in panel (b), the orange ellipses mark earlier episodes with plasmoids visible in the Ca II K blue wing. Colored markers in panel (e) indicate the location of $\tau = 1$ of the corresponding Ca II K spectral features in panel (b), the peaks at −29, −16, and −3 km/s (green, dark blue, and pink markers) are caused by different plasmoids. Scan the QR code on this poster or go to http://folk.uio.no/rouppe/plasmoids_chromis/ to view movies of panels (c), (e), (f), and (g).
More details about the simulation can be found in Nóbrega-Siverio et al. 2017.

Fig.3: non-Gaussian Si IV 1394Å profiles in a UV burst

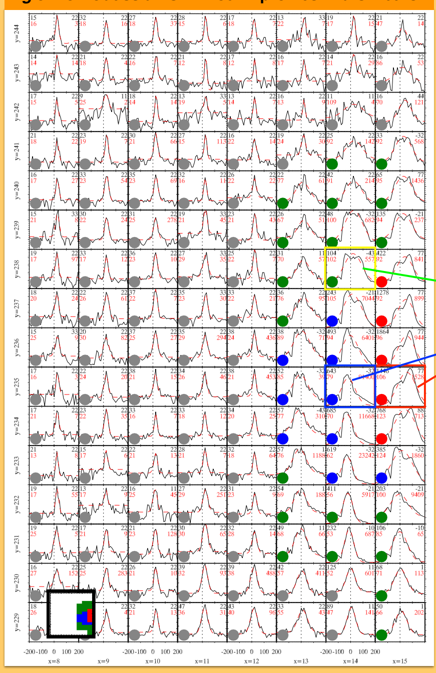

All Si IV 1394Å profiles in the IRIS raster region centred on the UV burst of the middle row in Fig. 2. The top left number is the maximum counts value, the top right number is the Doppler offset of this maximum in km/s. The red dashed line is a single Gaussian fit to the profile, the left red number is the Gaussian width in km/s, the right red number is the χ^2 value of the fit. The coloured circle marks the identification of the profile: blue/red if there is a dominant blue/red component, green for non-Gaussian profile (note that green is yellow in Fig. 2), grey for weak profiles (narrow and low maximum). x,y coordinates in IRIS raster index values.

Fig. 2: non-Gaussian Si IV profiles in UV bursts: these have been linked magnetic reconnection driven by the plasmoid instability (see e.g. Innes et al. 2015 and Guo et al. 2018). Where we observe non-Gaussian Si IV profiles, we see plasmoid-like blobs in Ca II K.

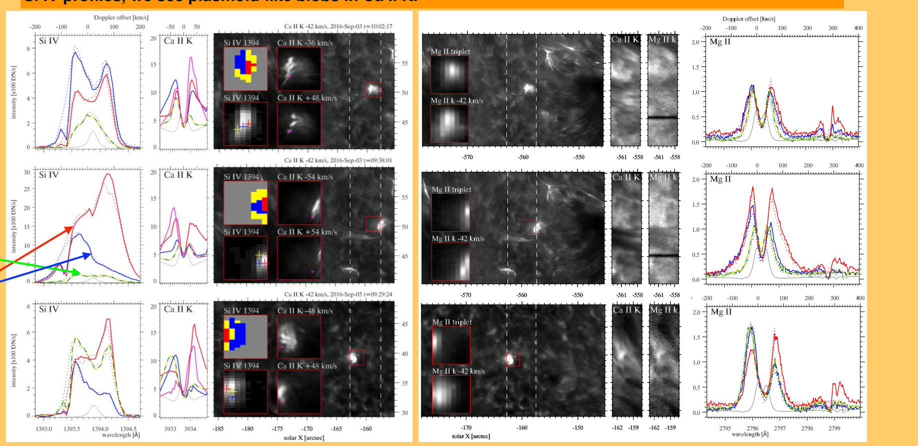

UV burst spectral profiles and diagnostics.The left two panels show spectral profiles at 3 different spatial locations marked with 3 different colors: blue, red and green/yellow, all recorded during the same IRIS raster time. The 3 different spatial locations are in close proximity of each other, their locations are marked with crosses in the inset Si IV raster maps in the 3rd column panels. The solid lines in the left panels are for Si IV 1394Å, the dotted lines are Si IV 1403Å profiles, shifted in wavelength and multiplied with a factor 2 to compensate for the difference in the atomic transition's oscillator strength. The 2nd column panels show Ca II K profiles in arbitrary units and averaged over the IRIS pixel. The pink profile is from a CHROMIS pixel in a plasmoid marked with a pink cross in the Ca II K insets in the 3rd column panels. The thin grey profiles are average spectral profiles for reference, the average Si IV 1394Å profile is multiplied with a factor 10 for clarity. The wide 3rd column panel is a Ca II K wing reference image, the vertical dashed lines mark the IRIS raster extent. The red box outlines the region for which inset images are shown at higher magnification. The lower left Si IV 1394Å map is integrated intensity over the full spectral window, in the top left map colours mark Si IV profile classification: red/blue pixels have strong (> 30 km/s) red/blue shifted components, yellow have broad or triangular non-gaussian profiles, see Fig. 3 for more detailed profiles.

The 4 columns on the right provide context information about the UV bursts from the Mg II lines. The Mg II h & k lines have strongly broadened central emission peaks and enhanced emission in the subordinate lines around 2799 Å. This indicates that the UV burst and associated heating is occurring rather deep in the atmosphere. The Mg II k3 & h3 cores are very dark - darker than the reference profile. The Ca II K3 and Mg II k3 raster images in the middle illustrate that the UV burst is happening below the fibrils and surge. The Si IV emission from the UV burst is also originating from this deep atmospheric region: the Si IV 1394 Å lines show a prominent Ni II absorption blend in the blue wing - this line is formed in cooler regions above the UV burst. Further note that the two Si IV lines differ by a factor ~2 - a property that can be explained by line formation under optically thin conditions. At the same time, the Mg II h & k lines have virtually identical strength and shape (the Mg II h line is overplotted as dashed lines), despite having a factor 2 difference in oscillator strength. This is typical for formation under optically thick conditions. For more details on the intriguing properties of UV burst spectral lines, see e.g., Vissers et al. 2015 and Peter et al. 2014. For a recent review on UV bursts, see Young et al. 2018.

IRIS-9, Göttingen, 25-29 June 2018

Poster

2. Chromospheric heating and dynamics

Intermittent reconnection and plasmoids in UV bursts in the low solar atmosphere

Luc Rouppe van der Voort[1], Bart de Pontieu[2,1], Göran Scharmer[3], Jaime de la Cruz Rodriguez[3], Juan Martinez-Sykora[2,4], Daniel Nobrega-Siverio[5,6], Lijia Guo[2,4], Sahin Jafarzadeh[1], Tiago Pereira[1], Viggo Hansteen[1], Mats Carlsson[1], Gregal Vissers[3]

[1]*Rosseland Centre for Solar Physics, University of Oslo*
[2]*Lockheed Martin Solar & Astrophysics Lab*
[3]*Institute for Solar Physics, Stockholm University*
[4]*Bay Area Environmental Research Institute*
[5]*Instituto de Astrofísica de Canarias*
[6]*University of La Laguna, Tenerife*

Magnetic reconnection is thought to drive a wide variety of dynamic phenomena in the solar atmosphere. Yet the detailed physical mechanisms driving reconnection are difficult to discern in the remote sensing observations that are used to study the solar atmosphere. We exploit the high-resolution instruments Interface Region Imaging Spectrograph (IRIS) and the new CHROMIS Fabry-Perot instrument at the Swedish 1-m Solar Telescope (SST) to identify the intermittency of magnetic reconnection and its association with the formation of plasmoids in so-called UV bursts in the low solar atmosphere. The Si IV 1403A UV burst spectra from the transition region show evidence of highly broadened line profiles with often non-Gaussian and triangular shapes, in addition to signatures of bidirectional flows. Such profiles had previously been linked, in idealized numerical simulations, to magnetic reconnection driven by the plasmoid instability. Simultaneous CHROMIS images in the chromospheric Ca II K 3934A line now provide compelling evidence for the presence of plasmoids, by revealing highly dynamic and rapidly moving brightenings that are smaller than 0.2 arcsec and that evolve on timescales of order seconds. Our interpretation of the observations is supported by detailed comparisons with synthetic observables from advanced numerical simulations of magnetic reconnection and associated plasmoids in the chromosphere. Our results highlight how subarcsecond imaging spectroscopy sensitive to a wide range of temperatures combined with advanced numerical simulations that are realistic enough to compare with observations can directly reveal the small-scale physical processes that drive the wide range of phenomena in the solar atmosphere.